1. THE DETERMINATION OF CRYSTAL AND MAGNETIC STRUCTURES

Since one may build a modest library of books on crystallography, X-ray diffraction and thermal neutron scattering it is rather impossible to achieve completeness or originality within the scope of one introductory chapter in a thesis. However, one may not assume that solid state physicists are thoroughly familiar with the field of crystal structure analysis. Therefore it is envisaged to outline this very useful branch of science, especially the technique of thermal neutron scattering by powder samples, in so far as is necessary to understand the results obtained. It is hoped that the power and the limitations of the method will be demonstrated in the reports of the investigations contained in the present work.

There is a natural way of partitioning the material to be presented. First we shall concentrate on the ideas involved; then an account will be given of the experimental setup, and lastly the focus will be on the processing of the results of the measurement.

1.1 The ideas

Diffraction is defined as the coherent and elastic scattering of a wave. Coherence means that there is a phase relation between the incident and the scattered wave; elastic scattering indicates that there is momentum transfer but no energy transfer between the wave and the scatterer.

Neglecting the diffraction by liquids, gases and amorphous solids, interesting though they are, we shall limit ourselves to scattering by crystalline solids.

For the present purpose we may take a crystal to be an infinite assembly of atoms showing translational symmetry in three dimensions. It is then possible to choose primitive translation vectors $\vec{a}$, $\vec{b}$ and $\vec{c}$ such that the crystal is invariant for a translation over any linear combination of

integral multiples of these vectors. By considering all the atoms in the crystal one may prove that the momentum transfer in the diffraction process, $\hbar\vec{\kappa}$, is discrete and can be written as

$$\vec{\kappa} = 2\pi\vec{\tau}$$

in which $\vec{\tau}$ is a vector of the reciprocal lattice:

$$\vec{\tau} = h\vec{a}^* + k\vec{b}^* + l\vec{c}^*$$

with integral h, k, l. The basis vectors of reciprocal space, $\vec{a}^*$, $\vec{b}^*$ and $\vec{c}^*$ are defined by 9 relations such as $\vec{a}\cdot\vec{a}^* = 1$ and $\vec{a}\cdot\vec{b}^* = 0$. These defining equations link the real "direct" space and the reciprocal, momentum space of the crystal.

When we express $\vec{\kappa}$ in the deflection angle 2θ and the wavelength λ, and relate $\vec{\tau}$ to an interplanar spacing d, the familiar Bragg law results: $|\vec{\kappa}| = 4\pi \sin\theta/\lambda$; $d = |\vec{\tau}|^{-1}$; $\lambda = 2d(hkl)\sin\theta(hkl)$. Therefore, the direction of a Bragg-reflection or diffraction peak is determined by the vectors $\vec{a}^*$, $\vec{b}^*$, $\vec{c}^*$ and the numbers h, k, l.

One may further show that the intensity of a reflection is determined by h, k, l and the contents of the unit cell defined by $\vec{a}$, $\vec{b}$ and $\vec{c}$. Consider N point scatterers ("atoms") in the unit cell, the jth atom having the average position $\vec{r}_j = x_j\vec{a} + y_j\vec{b} + z_j\vec{c}$, and scattering a wavelet with amplitude b_j. Their combined effect is then a wave with amplitude

$$F(\vec{\kappa}) = \sum_j b_j \exp i\vec{\kappa}\cdot\vec{r}_j$$

The function $F(\vec{\kappa})$ is recognized as a Fourier transform. This becomes even clearer when we formally define a "continuous" scattering density distribution function as a sum of delta-functions [+]:

$$b(\vec{r}) = \sum_j b_j \delta(\vec{r}-\vec{r}_j)$$

and write $F(\vec{\kappa})$ as

$$F(\vec{\kappa}) = \int_{cell} b(\vec{r}) \exp i\vec{\kappa}\cdot\vec{r}\, d\vec{r}$$

[+] The Dirac delta-function is defined by the expressions $\delta(x) = 0$ for $x \neq 0$, $\delta(x) = \infty$ for $x = 0$, and $\int_{-\infty}^{+\infty}\delta(x)\,dx = 1$. It has the property $\int_{-\infty}^{+\infty} f(x)\,\delta(a-x) = f(a)$ and can be Fourier-transformed as $\delta(x) = \frac{1}{2\pi}\int_{-\infty}^{+\infty} e^{-ikx}\,dx$. The three-dimensional $\delta(\vec{r})$ is defined as $\delta(\vec{r}) = \delta(x)\,\delta(y)\,\delta(z)$.

Crystallographers call $F(\vec{\kappa})$ the structure factor and write it as

$$F(hkl) = \sum_j b_j \exp 2\pi i (hx_j + ky_j + lz_j).$$

Omitting at present several factors, continuous in θ, arising from the geometry of the experiment, the scattered intensity is proportional to the square of the amplitude:

$$I(hkl) \sim |F(hkl)|^2$$

This poses the central problem in a crystal structure determination: the information available by experiment contains the magnitude of the structure factor F, not its complex phase angle. This prohibits us to perform the inverse Fourier transformation yielding the scattering density:

$$b(\vec{r}) = \frac{1}{(2\pi)^3} \sum_{\vec{\kappa}} F(\vec{\kappa}) \exp - i \vec{\kappa} \cdot \vec{r}$$

or, equivalently,

$$b(\vec{r}) = \frac{1}{(2\pi)^3} \sum_{h,k,l} F(hkl) \exp - 2\pi i (hx + ky + lz)$$

In order to find $b(\vec{r})$ we must guess the phase of F by approximately solving the structure, for which several techniques are available.

Now having outlined an abstract formalism describing scattering of a "wave" by a "crystal", the next step is to specify the nature of the wave, the crystal and the interaction process.

First, the wave.

This is not the place to discuss the wave properties of the neutron. We limit ourselves to noting that thermal neutrons emerging from a reactor show an essentially maxwellian velocity distribution, the maximum of which corresponds to a wavelength λ of about 1.8 Å. This is the right order of magnitude for crystal structure analysis.

Second, the scattering potential.

Except gravitation, two types of force are known to which neutrons are sensitive. Of course, the first of these is the nuclear force acting between hadrons, and the second is the electromagnetic force acting on the neutron spin.

Third, the crystal.

Due to nuclear interaction the neutron beam will be subject to scattering by the nuclei. In this case the assumption of point scatterers is valid, because the size of the nucleus is very small compared to the neutron wavelength.

Since no detailed theory of nuclear interaction is available at present there is no way to calculate the scattering lengths b for the isotopes. Values of b have been determined by experiment; they are of the order of 10^{-12} cm and can be positive, negative and complex.

In the case of magnetic scattering a number of things change. The electromagnetic force is active between the magnetic moment γ of the neutron spin and the magnetic moment μ of the atoms in the crystal.

Since the spatial extent of electron wave functions is of the same order of magnitude as the neutron wavelength, magnetic atoms cannot be described as point scatterers. This is accounted for by the introduction of the magnetic form factor $f(\vec{\kappa})$, the Fourier transform of the electron wave functions centred at the nucleus. These have been calculated and tabulated for 3d metals and lanthanides, [26] and [45].

Moreover, since the magnetic moment $\vec{\mu}$ is a vector quantity the Fourier transform of the magnetic scattering density is also a vector quantity:

$$\vec{F}_M(\vec{\kappa}) = b_M \sum_j \vec{\mu}_j f_j(\vec{\kappa}) \exp i \vec{\kappa} \cdot \vec{r}_j$$

where b_M is the scattering length of a magnetic moment of 1 Bohr magneton; the calculated value is

$$b_M \equiv \frac{e^2}{2mc^2} \gamma = 0.2695 \times 10^{-12} \text{ cm.}$$

Lastly, the magnetic interaction is not isotropic: the scattered intensity depends on the polarization of the neutron spin and on the direction of $\vec{\kappa}$ with respect to $\vec{F}_M$. For unpolarized neutrons the scattered intensity can be written as:

$$I_M(\vec{\kappa}) \sim |\vec{F}_M(\vec{\kappa})|^2 - \frac{|\vec{\kappa} \cdot \vec{F}_M(\vec{\kappa})|^2}{|\vec{\kappa}|^2}$$

This implies that only the component of $\vec{F}_M$ perpendicular to $\vec{\kappa}$ contributes to the magnetic scattering. This is a most useful property since it enables one to determine the direction of the magnetic moments with respect to the crystal axes $\vec{a}$, $\vec{b}$ and $\vec{c}$. In a powder experiment certain limits are set by the symmetry of the magnetic structure. In a cubic magnetic symmetry the magnitude only of $\vec{\mu}$ can be determined in a powder experiment; in a uniaxial (tetragonal, hexagonal or trigonal) magnetic symmetry the components parallel and perpendicular to the unique axis can be determined.

It remains to be noted that for unpolarized neutrons there is no coherence, i.e. no interference, between magnetic and nuclear scattering: the intensities are simply additive. This is usually a handicap in the investigation of a ferromagnet, for which nuclear and magnetic scattering peaks coincide.

It will be clear that this presentation is rather crude and far from complete. In a sophisticated derivation of scattering cross sections one

should apply a formal quantum mechanical theory of scattering [1]. Furthermore, symmetry properties other than translational are ignored, whereas in fact the establishment of symmetry relations between atoms in the unit cell, if they exist, is an essential step in any crystal or magnetic structure analysis [2].

Moreover, a number of important processes occurring in real crystals were completely neglected [3]. The most important of these for a diffraction experiment are thermal vibrations and absorption.

Due to thermal motion the jth atom appears to the neutron as located at an instantaneous position $\vec{r}'$ differing from its mean value $\vec{r}$ by a vector $\vec{u}_j$. As a result an additional phase factor $\exp i\vec{\kappa} \cdot \vec{u}_j$ is introduced in the structure factor expression that is increasingly important at higher scattering angles. For an evaluation of the total effect the individual phase differences must be averaged over the crystal, and this leads to the Debye-Waller factor. In its simplest form equal mean square displacements are assumed for all atoms, from which one derives a factor in the intensity equal to $\exp -\frac{1}{3}\langle\vec{u}^2\rangle\vec{\kappa}^2$, usually written as $\exp -2B \sin^2\theta/\lambda^2$. If the measurements are extended to sufficiently high values of $\vec{\kappa}$, one may determine the differences in $\langle\vec{u}^2\rangle$ for different atoms, or even anisotropic values.

The influence of absorption on the measured intensity is not so easily evaluated in a general case. Absorption effects are very sensitive to the geometrical shape of the specimen and its orientation, since the mean path of a neutron in the sample is the relevant quantity. In the case of a cylindrical specimen shape, as is usually employed, the results of numerical calculations have been tabulated; however, experience shows that, when no absorption correction is carried out the parameters for the thermal motion are decreased with respect to their expected values, whereas the structure parameters are not affected by the neglect of absorption effects.

1.2 The instrument

The type of instrument commonly used for single crystal and powder diffraction, when no energy or polarization analysis is carried out, is a two-axis spectrometer using a constant beam of monochromatized neutrons. It is designated two-axis since the neutrons are deflected twice, once by the monochromator and once by the sample prior to being detected in the counting system.

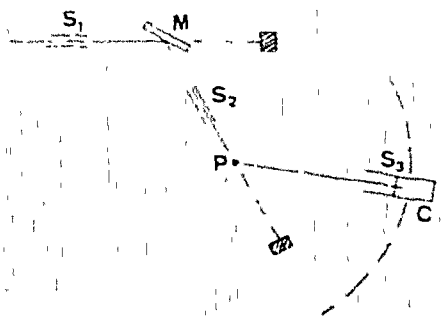

Fig. 1 Schematic drawing of a powder diffractometer.

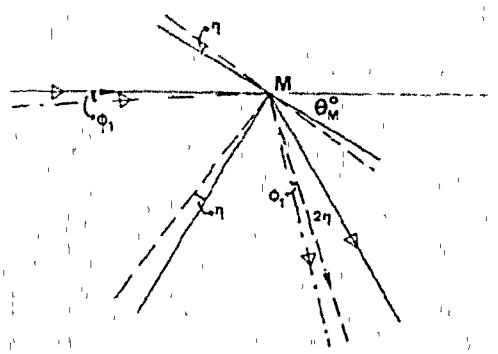

Fig. 2a The monochromatization process.

For single crystal work a mechanism is required to orient the crystal in any desired position, in order to bring any scattering vector in the horizontal plane where the neutrons can be counted. For a powder specimen no such mechanism is required, since all crystal orientations are available. As a consequence the two-axis powder diffractometer is the simplest type of neutron spectrometer, measuring scattered intensity as a function of scattering angle only.

In order to formulate criteria for a good spectrometer it is necessary to understand its "optical" properties. A complete treatment, though for a slightly idealized case, was given by Caglioti et al. in a number of papers that appeared around 1958. Their analysis of the powder diffractometer [4] was the starting point for the design of the spectrometer at the HFR at Petten and for the method of analysis described in section 3.

A schematic drawing of the instrument is presented in fig. 1.

Apart from other radiation, a beam of thermalized neutrons emerges from the reactor through a slit system S_1. It is diffracted by the monochromator crystal M. The scattered neutrons are taken off at an angle $2\theta_M$, defined by slit system S_2, which results in a beam with a narrow wavelength band. The sample P is bathed in the once deflected beam, and the scattered neutrons are detected by a counter moving on an arc centred at the sample position. In front of the detector a third slit system S_3 is placed.

The slit systems have finite apertures and the monochromator has a finite mosaic structure. In order to find the peak shape and luminosity, we must follow the path of neutrons that deviate in initial direction and in wavelength from the so-called central ray. In doing so we shall restrict ourselves to the plane in which the scattering takes place, i.e. we assume perfect vertical collimation.

The monochromatization process is shown in fig. 2a.

A neutron passing S_1 at an angle ϕ_1 with respect to the mean direction, and with a wavelength $\lambda = \lambda_o + \Delta\lambda$, will select a crystal mosaic block at an angle η with respect to the mean of the distribution, such that $\lambda = 2\, d_M \sin(\theta_M^o + \eta + \phi_1)$. It will be scattered in the direction $2\theta_M = 2\,\theta_M^o + 2\eta + \phi_1$.

The incoming direction of the neutron is described by the parameter ϕ_1; the wavelength shift $\Delta\lambda$ is related to $\Delta\theta_M \equiv \eta + \phi_1 = \delta$ by the expression

$$\Delta\lambda = 2\, d_M \cos\theta_M^{\circ} \times \delta,$$

as is evident by differentiation of Bragg's law.

The scattering by the specimen is illustrated in fig. 2b.

The neutron with initial parameters (ϕ_1, δ) now travels at an angle $\phi_2 = 2\theta_M - 2\theta_M^{\circ} = 2\eta + \phi_1$ with respect to S_2. The Bragg angle at the sample will be $\theta_P = \theta_P^{\circ} + \zeta$, with ζ to be determined, so that for the geometry shown in fig. 2b the neutron will be scattered in the direction $2\theta_P^{\circ} + 2\zeta - \phi_2$. The minus sign is a direct consequence of the geometry chosen; if the twice reflected beam would be chosen according to the dotted line in fig. 1. the + sign would be appropriate. This is the well-known focussing property of the so-called parallel geometry.

The parameter ζ is related to the neutron wavelength and must therefore be related to δ; the relation is:

$$\Delta\lambda = 2\, d_M \cos\theta_M^{\circ} \times \delta = 2\, d_P \cos\theta_P^{\circ} \times \zeta$$

whence

$$\zeta = \frac{d_M \cos\theta_M^{\circ}}{d_P \cos\theta_P^{\circ}} \times \delta = \frac{\mathrm{tg}\,\theta_P^{\circ}}{\mathrm{tg}\,\theta_M^{\circ}} \times \delta \equiv p \times \delta$$

where $p = \mathrm{tg}\theta_P^{\circ} / \mathrm{tg}\theta_M^{\circ}$

As stated, the neutron travels in the direction $2\theta_P^{\circ} + 2\zeta - \phi_2 \equiv 2\theta_P^{\circ} + \phi_3$ with $\phi_3 = 2\zeta - \phi_2$; if the counter is at the position $2\theta_P^{\circ} + \rho$ the neutron travels at an angle $\phi_3 - \rho$ with respect to S_3.

In order to calculate the peak shape and integrated intensity as a function of ϕ_1, δ and ρ we must introduce the probability that a neutron traveling at an angle ϕ_i with respect to S_i will be transmitted, and the probability for the mosaic angle η of the monochromator to be available. In the ideal case all orientations are equally probable in the powder.

As is shown by experiment, the transmission function of a Soller slit S_i may be described to a good approximation by a gaussian:

$$P_i(\phi_i) \sim \exp - \phi_i^2 / \alpha_i^2$$

where α_i is a measure of the aperture of S_i; moreover the distribution function of mosaic blocks may be approximated by a gaussian:

$$P_M(\eta) \sim \exp - \eta^2 / \beta^2$$

where β is related to the mosaic spread of the monochromator. The distribution

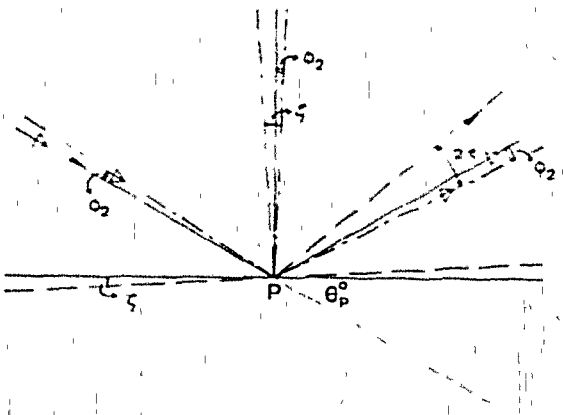

Fig. 2b Scattering by the sample.

function for the whole spectrometer is then found as the product of the individual transmission functions:

$$P(\phi_1, \delta, p, \rho) \sim \exp - \left[\phi_1^2/\alpha_1^2 + \eta^2/\beta^2 + \phi_2^2/\alpha_2^2 + (\phi_3 - \rho)^2/\alpha_3^2 \right]$$

Integration over ϕ_1 and δ yields the peak shape I (ρ); a final integration over ρ yields the integrated intensity, i.e. luminosity, as a function of p.

Carrying out the integrations Caglioti et al found the peak shape I(ρ) to be a gaussian function with peak width W

$$I(\rho) \sim \exp - \rho^2 / W^2;$$

the proportionality factor being a function of the α_i, β and p but not of ρ. The peak width W is determined by

$$W^2 = A\, p^2 + B\, p + C$$

where A, B and C are functions of the α_i and β:

$$A = 4\, \frac{\alpha_1^2\, \alpha_2^2 + \alpha_1^2\, \beta^2 + \alpha_2^2\, \beta^2}{\alpha_1^2 + \alpha_2^2 + 4\beta^2}$$

$$B = -4\, \frac{\alpha_1^2\, \alpha_2^2 + 2\alpha_2^2\, \beta^2}{\alpha_1^2 + \alpha_2^2 + 4\beta^2}$$

$$C = \alpha_1^2 + \frac{\alpha_1^2 \alpha_2^2 + 4\alpha_1^2 \beta^2}{\alpha_1^2 + \alpha_2^2 + 4\beta^2}$$

For the luminosity L is found:

$$L = \frac{\alpha_1 \alpha_2 \alpha_3 \beta}{(\alpha_1^2 + \alpha_2^2 + 4\beta^2)^{\frac{1}{2}}}$$

L might be called the optical luminosity of the spectrometer. In the [illegible] a number of other factors contribute as well. The first of these is the monochromator peak reflectivity, i.e. the probability that an incident neutron is diffracted at all by the monochromator. Then there is the probability that a neutron will be Bragg-scattered at all in the particular reflection (hkl) at θ_o, viz. F(hkl), the quantity to be measured. Absorption in the monochromator, the sample or the surrounding air will reduce the countrate, and a further reduction will occur due to a non-100% efficiency of the counting system.

Moreover, the crystallites are arranged at random; calculation of the fraction oriented such that neutrons diffracted by them will reach the counter, leads to the Lorentz factor $1/\sin\theta \sin 2\theta$.

Finally, the influence of vertical divergence. Since for a spherical sample the paths of diffracted neutrons form a cone, the segment of the cone intercepted by the counter surface bears a direct relation to the countrate. For low angles this will lead to a marked asymmetry of the peak; however, in first approximation this does not lead to a change in the Lorentz factor. In cylindrical samples the diffraction cone is convoluted with the sample height, which at low θ leads to a broadened but more symmetric peak.

Caglioti et al. give numerous examples of particular combinations of α_i's and β, illustrating the effect of variation of one or more parameters. One may draw the following general conclusions:

a) resolution is not a sensitive function of the monochromator's mosaic spread, whereas L increases with increasing β, so that β should be made as large as possible. Since monochromators are usually far too perfect crystals this has led to many investigations with respect to the performance of monochromator crystal materials.

b) over the range of p covered in actual experiments the resolution is not a sensitive function of α_2. In fact the crude natural collimation of about 1^o provided by the ratio of sample diameter to its distance from the monochromator is quite sufficient. For this reason most powder

spectrometers operate without an explicit slit system S_2.

c) since the luminosity is linear in α_3, perhaps the easiest way of increasing the countrate is by increasing α_3. However, since α_3 appears in the constant term of the resolution function W the loss in resolution, particularly at low p, is considerable.

d) resolution should be improved very much by choosing a large d_M, resulting in a lower p for the reflections of interest. This will be discussed below.

Lastly, from the geometry of the monochromatization process it is evident that the crystal, set at an angle θ_M for a reflection hkl at wavelength λ_o is also in reflection position for nh, nk, nl at wavelength λ_o/n. In order to reduce λ/n contamination in the once deflected beam powder spectrometers are usually designed to operate at a wavelength near 1 Å.

When the spectrometer at the High Flux Reactor at Petten was designed it was considered revolutionary, being based on a new interpretation of the work by Caglioti et al.

Loopstra showed [5] that the proper way to gain resolution is by increasing θ_M, at constant d_M, thereby operating at a relatively long wavelength. In doing so one moves over the maximum in the wavelength distribution, such that there are fewer neutrons of the selected wavelength λ_o and more of the unwanted $\lambda_o/2$ available in the beam coming from the reactor. Thus, the use of an appropriate filter is essential. Pyrolytic graphite is suitable, more than other filter materials, since it has a transparancy window in the region $2.3 < \lambda < 2.9$ Å *).

Moreover, it is possible to make up for the decrease in primary flux by a number of cooperating factors such as increased reflectivity of the specimen at longer λ, better efficiency of the counter, and positive use of vertical divergence through a short distance between specimen and counter.

---

*) The material consists of hexagonal crystallites that have their c axis aligned in a normal mosaic distribution, but whose a and b axes are oriented at random in the plane $\perp \vec{c}$. When the neutrons are incident $\| \vec{c}$ they will be (Bragg)scattered except when their wavelength does not match a Bragg-angle.

The validity of this approach has been proved by the performance of the spectrometer at Petten during its years of operation. In its normal configuration, operating at λ = 2.57 Å obtained from a Cu (111) crystal at $2\theta_M = 76^o$, with a total thickness of 10 cm pyrolytic graphite as a $\lambda/2$ filter, and 30' slits S_1 and S_3, it compares favourably with other spectrometers. Its resolution and peak to background ratio are very good while maintaining a comparable countrate (per unit of central thermal flux in the reactor core), resulting in a standard measurement time of two days for a 10 cm^3 sample.

1.3 Data reduction

In section 1 of this chapter it was noted that the result of a measurement consists of the magnitudes of Fourier coefficients of the scattering density in the unit cell, and that the art of structure analysis consists in reconstructing the phase angles of these Fourier coefficients. This analysis is not always straight-forward.

In fig. 3 some results are shown. For three different compounds the measured diagram is given by the dots, representing the actual counts assembled as a function of scattering angle 2θ (the experimental unit of angle, dmc, is such that 10^4 dmc ≡ 360^o). The drawn line in each diagram represents the result of the calculations to be described.

If nothing is known at all about the crystal structure of the compound, the first step is to try and find the unit cell, i.e. the vectors $\vec{a}^*$, $\vec{b}^*$ and $\vec{c}^*$ such that each peak in the diagram can be represented by three integer numbers hkl with $|\vec{\kappa}| = 4\pi \sin\theta/\lambda = |h\vec{a}^* + k\vec{b}^* + l\vec{c}^*|$.

The second step is the determination, if possible, of the full symmetry of the crystal structure [2]. The distinction between mirror planes and rotation axes, or the establishment of a centre of symmetry is only possible by statistical analysis. However, glide planes and screw axes manifest themselves through systematic extinction of certain types of reflections. In a minority of cases a unique allocation of the space group is possible by determination of the reflection conditions, notably when screw axes and/or glide planes are present. When no reflection conditions are found one knows that screw axes and glide planes are absent, but one has no information about the

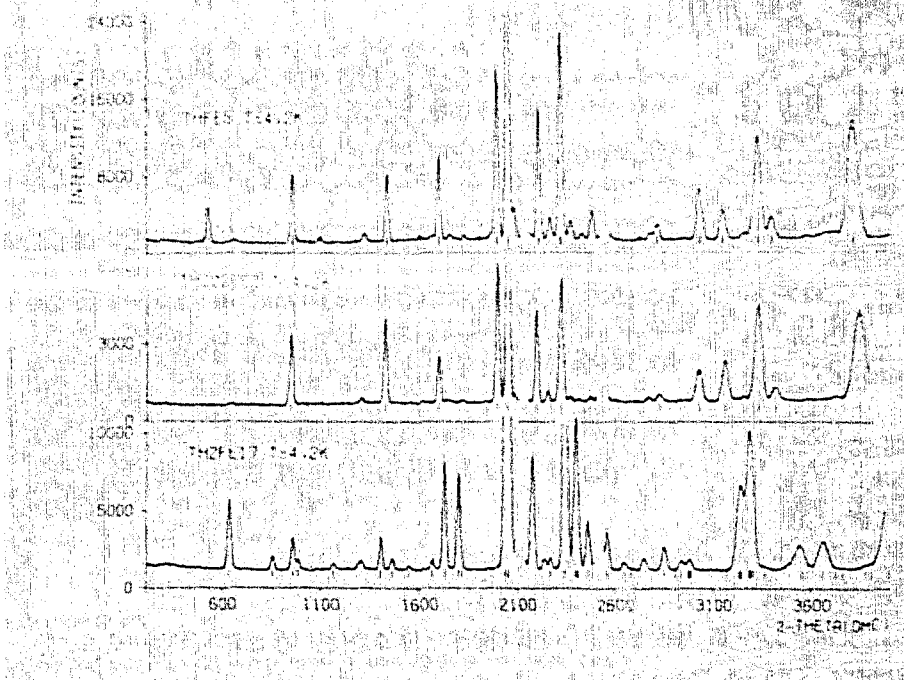

Fig. 3. Examples of powder diffraction diagrams.

existence of rotation axes and mirror planes. In this latter case one has to keep the possible combinations of these in mind until the very end of the investigation.

When the unit cell is known one may determine how many formula units it contains by calculating the resultant density. The condition that this number is integral and compatible with the symmetry found, together with some idea about the actual density, is usually sufficient. Then one may attempt a shrewd guess at the structure, or proceed by more sophisticated techniques, to arrive at a structure model. It would go too far to attempt to give a detailed description of these techniques, since they depend on having a large number of structure factor magnitudes available, and in a powder diffraction experiment they can hardly be used. Most of them make use of the fact that relations must exist between structure factors, since their number is far greater than the number of parameters, i.e. the atomic coordinates. For instance, the phase of a reflection (nh, nk, nl) is determined as soon as the phase of (hkl) is specified. Moreover, it occurs only very rarely that the analysis described so far has not been carried out prior or parallel to the neutron diffraction experiment, by an X-ray single crystal investigation.

So in the usual case the crystal structure is known in more or less detail. When determining a magnetic structure a similar analysis must be carried out in order to arrive at a model for the magnetic structure.

The final stage of the analysis consists of a least squares refinement of the trial structure in order to minimize the disagreement between the structure factors calculated for the model and the observed values.

The residual misfit in the least squares minimum is usually evaluated [illegible] I_{obs} [illegible] I_{calc} [illegible] the observed and calculated integrated intensity in a reflection, the so-called R-factor is defined as

$$R = 100 \times \frac{\sum_{\kappa} | I_{obs}(\kappa) - I_{calc}(\kappa) |}{\sum_{\kappa} I_{obs}(\kappa)}$$

Here we can no longer avoid to mention a problem, circumvented so far, inherent in the powder method: overlap of neighbouring reflections. Until now we tacitly assumed that all structure factor magnitudes were measured independently, as can be done in a single crystal investigation. In a powder investigation this can only very seldom be realized. Since the scattered intensity is determined as a function of the magnitude of $\vec{\kappa}$ the number of reflections in a κ-interval increases with increasing $|\vec{\kappa}|$, so that overlap of neighbouring reflections must occur inevitably for some value of $|\vec{\kappa}|$, whatever the resolution is.

However, there is a solution to this difficulty: it was demonstrated in section 2 that the peak shape is gaussian, with a known functional form of the half width. At every measured point we may therefore calculate the contribution of each reflection adding to the total count at that point, and use the point by point measured intensities, rather than integrated intensities, in the least squares refinement, thereby making full use of the information available. This method of analysis [6], as opposed to estimating the area under a diffraction peak, is called profile analysis.

The limitation of this method is set by the determination of the background count, which must be subtracted before the refinements are carried out.

Part of the background count may be described by analytic functions, namely the incoherent and inelastic scattering, if known. However, the count due to neutrons swarving in the reactor hall, or possibly other radiation picked up by the counter, and any contribution from sample holder,

ervostat and cooling liquids must be determined by analysis of the actual countrate. In diagrams with much overlap there are insufficient regions where the background level can be determined with confidence.

The wide applicability of the profile refinement method revives the old dilemma between resolution and intensity. In the case of high resolution, but poor intensity, the individual structure factors are known with limited accuracy. This is a favourable situation in the sense that one needs to perform an analysis from the very beginning, in order to be able to "play around" with the structure factors. On the other hand it is a very unfavourable situation when several structure models exist that differ in relative intensities only, as e.g. when one must discern between rotation axes and mirror planes or between a centrosymmetric or non-centrosymmetric structure.

The other extreme is a very high countrate, and therefore good accuracy, obtained with poor resolution. If a reliable model is available, this can be refined very well; if on the other hand the model proves to be incorrect one does not have the means to search for a better one.

Both extreme cases are clearly to be avoided, and the optimum experimental conditions must be sought somewhere between the two. It would be useful to develop criteria, if possible, from which one may derive the required countrate and resolution for a particular investigation.